Applied Surface Science 280 (2013) 556–563

Contents lists available at SciVerse ScienceDirect

Applied Surface Science

journal homepage: www.elsevier.com/locate/apsusc

Enhancing mechanism of visible-light absorption for photovoltaic response and photoluminescence of Zn_2SnO_4 with high solubility of Bi^{3+}

Xiansheng Liu[a], Junqiao Wang[a], Erjun Liang[a,*], Weifeng Zhang[b]

[a] School of Physical Science & Engineering, Key Laboratory of Materials Physics of Ministry of Education of China, Zhengzhou University, Zhengzhou 450052, China

[b] Institute of Micro-system Physics, Key Laboratory of Photovoltaic Materials of Henan Province, School of Physics & Electronics, Henan University, Kaifeng 475001, China

ARTICLE INFO

Article history:
Received 25 December 2012
Received in revised form 25 April 2013
Accepted 7 May 2013
Available online 14 May 2013

Keywords:
Codopant
Surface photovoltage
Photoluminescence
Electron transition

ABSTRACT

The enhanced visible-light absorption for photovoltaic response and room temperature photoluminescence of Bi^{3+}-doped Zn_2SnO_4 nanoparticles are studied. The valence states of Bi^{3+} and Zn^{2+}/Sn^{4+} are detected by their core level X-ray photoelectron spectra. Bi_{Zn}^{+} and Bi_{Sn}^{-} from substitutions of Bi^{3+} for Zn^{2+}/Sn^{4+} interattract and form noncompensated *n*–*p* codopant band to improve visible light absorption and facilitate electron transition for photovoltaic response and photoluminescence. Abundant surface states and weak built-in electric field near surface improve together the separation of photoinduced charges of *n*-type nanoparticle semiconductors. The investigation of high dopant solubility to enhance visible light absorption could be applied to other wide band gap ternary oxides.

1. Introduction

Due to weak absorption of long-wavelength photons of silicon and oxide semiconductor solar cells, intermediate band (IB) and noncompensated *n*–*p* codopant band (CDB) solar cells have been proposed for the third generation of photovoltaics [1–3]. According to IB theory, the IB can be obtained in standard semiconductors by the introduction of deep levels between valence band (VB) and conduction band (CB) from designing quantum dots or doping ions [4]. Ion-doping to construct IB is widely used in oxide semiconductor solar cells due to its simplicity. Whereas low dopant solubility usually hinders to construct IB to further improve visible light absorption of wide band gap ternary oxides. For CDB theory, band gap narrowing is caused by noncompensated anion–cation codoping and there is attraction between anion and cation substitutional ions. The Fe/Cr + N codoping usually selects the uni-metal oxides such as TiO_2 [2,3,5,6]. The investigation of Fe/Cr + N codoping TiO_2 triggers us to consider that noncompensated anion–cation codoping could be constructed by substitution trivalent ions (A^{3+}) for bivalent and quadrivalent ions (B^{2+}/C^{4+}) in ternary oxides such as $SrTiO_3$ and Zn_2SnO_4 (ZTO).

ZTO is an attractive *n*-type semiconductor with band gap 3.6 eV [7], which is only sensitive to ultraviolet light. A recent study reveals that ZTO has a lower rate of electron-hole recombination and longer lifetime of electrons comparing with TiO_2 in dye-sensitized solar cells [8]. Nevertheless, the photoelectric response of ZTO is not strong due to its weak visible light absorption [9,10]. To enhance the visible-light absorption of ZTO, so far, doping with S has been tried [11]. Visible light photocatalytic activity of ZTO was enhanced by S-doping. S^{4+} and S^{6+} are common valence states, however, Zn^{2+} and Sn^{4+} are the considered valence states in ZTO. The substitution S^{6+}/S^{4+} for Zn^{2+}/Sn^{4+} could not form interattraction between anion and cation to further enhance the dopant solubility. Therefore trivalent ions should be introduced to substitute Zn^{2+}/Sn^{4+} in ZTO, just like In^{3+}-doped Cd_2SnO_4 [12]. Dy^{3+} ions have been introduced to improve the photoluminescence (PL) and photocatalytic properties of ZTO [13], however, because of the high cost of rare earth ions of Dy^{3+}, the doping content is limited largely to further enhance visible light absorption. It is significant to use low cost trivalent Bi^{3+} ions, well-known sensitizer, to substitute Zn^{2+}/Sn^{4+} in ZTO.

In this paper, Bi^{3+}-doped ZTO were synthesized by hydrothermal method to enhance the visible light absorption of ZTO. The photogenerated charge separation and recombination behaviors on the surface of the samples are investigated by surface photovoltage spectroscopy (SPS) and electric field-induced surface photovoltage spectroscopy (EFISPS) as well as PL spectra.

---

[*] Corresponding author. Tel.: +86 371 67767838; fax: +86 371 67766629.
E-mail addresses: ejliang@zzu.edu.cn, liuxiansheng69@126.com (E. Liang).

0169-4332/$ – see front matter. Crown Copyright © 2013 Published by Elsevier B.V. All rights reserved.
http://dx.doi.org/10.1016/j.apsusc.2013.05.026

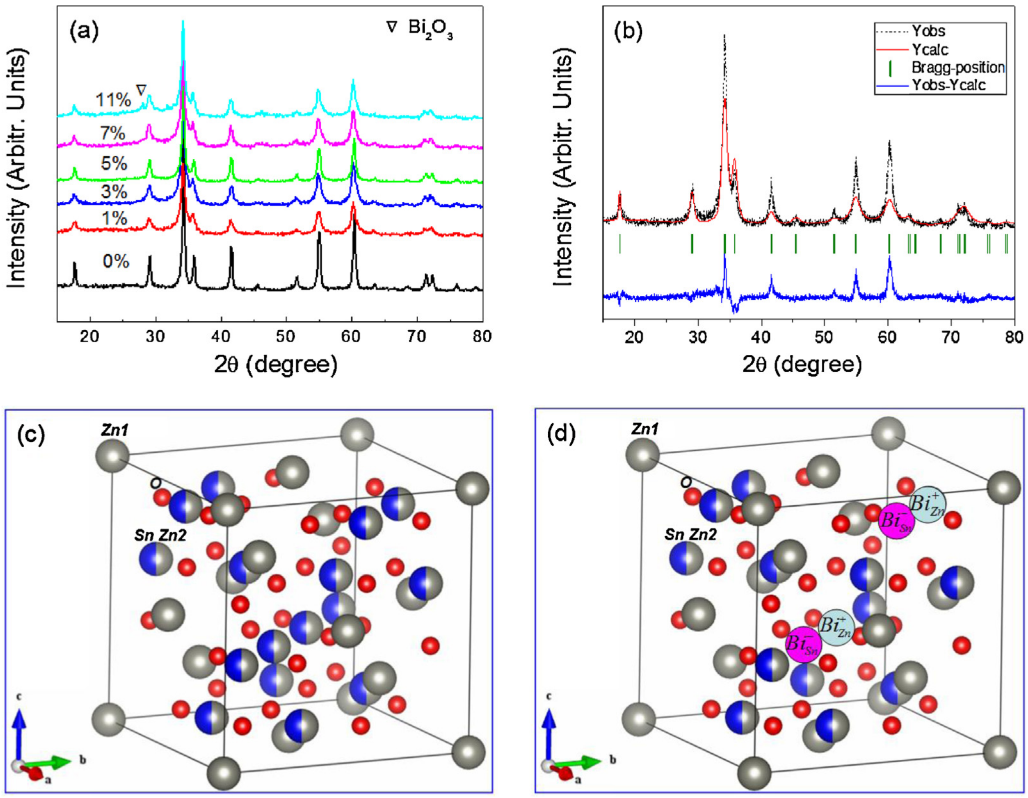

Fig. 1. (a) XRD patterns of pure and Bi^{3+}-doped ZTO with contents of 1, 3, 5, 7 and 11 mol%, respectively. (b) Structure refined results of Bi^{3+}-doped ZTO (3 mol%) with XRD data at room temperature. (c) and (d) Schematic diagram of lattice structures of ZTO and Bi^{3+}-doped ZTO, respectively (red spheres indicate O, gray spheres indicate Zn1, gray semi-spheres indicate Zn2, blue semi-spheres indicate Sn, Bi_{Zn}^{+} indicates Bi^{3+} substituting Zn^{2+}, and Bi_{Sn}^{-} indicates Bi^{3+} substituting Sn^{4+}). (For interpretation of the references to color in this figure legend, the reader is referred to the web version of the article.)

2. Experimental

ZTO samples with different contents of Bi^{3+} were synthesized with hydrothermal method. All the regents used were analytic grade. $ZnCl_2$ (6.4 mmol), $Bi(NO_3)_3{\cdot}5H_2O$ (certain amount) and $SnCl_4{\cdot}5H_2O$ (3.2 mmol) were dissovled into 20 mL water/ethylene glycol (1:1 volume ratio) mixed solvent. $N_2H_4{\cdot}H_2O$ was drop-wise added into the solution till pH = 10 and precipitation formed rapidly. After stirring for several minutes, the obtained slurry was transferred to a 100 mL autoclave and heated at 180 °C overnight. The autoclave was cooled to room temperature naturally. The supernatant fluid was discarded. The lower precipitation was rinsed with deionized water to remove residual cations and anions followed by drying at 80 °C for 2 h. Then the samples were sintered at 500 °C for 1.5 h in air to obtain the Bi^{3+}-doped ZTO nanoparticles.

X-ray diffraction (XRD) patterns were recorded on a DX-2500 diffractometer with Cu Kα radiation with $\lambda = 0.1542$ nm. X-ray photoelectron spectroscopy (XPS, AXIS Ultra^{DLD}) was used to detect binding energy change and valence states of elements. Raman spectra were obtained on a laser Raman spectrograph (LRS-III). The microstructures of the samples were recorded with a field emission scanning electron microscope (FE-SEM, Model JSM-6700F). The diffuse reflectance spectra were observed on a UV–vis spectrophotometer (Varian Cary 5000) with $BaSO_4$ as the standard reference and were converted to the absorbance data through the Kubelka–Munk method. The PL spectra were performed at room temperature with a Fluoromax-4 spetrofluorometer (HORIBA Jobin Yvon). SPS was carried out with a home-built apparatus and EFISPS was used a technique combining an electric field-effect principle with the SPS method. The samples were put in the middle of a sandwich structure composed of two pieces of ITO (indium tin oxide) glass. External electric field was applied to the two sides of samples and was regarded as positive when its direction was identical to that of incident light. The life time of photogenerated carriers is estimated with the life time of fluorescence on a PL spectroscopy (HORIBA, FL3-22).

3. Results and discussion

3.1. Crystal structure

Fig. 1a shows the XRD patterns of pure and Bi^{3+}-doped ZTO with Bi^{3+} contents of 1, 3, 5, 7 and 11 mol%, respectively. It is clear that the diffraction peaks correspond to a cubic structural zinc stannate (JCPDS No. 74-2184) and become weaker and wider after Bi^{3+} doping. The average grain sizes of pure and Bi^{3+}-doped (5 mol%) ZTO are estimated from the XRD patterns using Sherrer's equation with their strongest peaks to be about 27 and 17 nm, respectively, i.e. the average grain sizes of ZTO are within nano-scale and decrease obviously after Bi^{3+} ions doping. In addition, the diffraction peaks shift toward smaller angle after Bi^{3+}-doping, suggesting that the doping with Bi^{3+} leads to an increase in the lattice constant. Since all the XRD patterns were measured with powdered samples, the effects of sample height, effective X-ray transparency, mismatch strain, etc. on the peak shift can be excluded. Structure refinements (see Fig. 1b) of the XRD data using Rietveld method confirm the proposal. The lattice constants of ZTO with 0, 1, 3, 5, 7 and 11 mol% Bi^{3+} are obtained to be about 8.666, 8.692, 8.693, 8.694, 8.696, 8.698 Å, respectively. Since the radius of Bi^{3+} (0.103 nm) is larger than those of Sn^{4+} (0.069 nm) and Zn^{2+} (0.074 nm), substitutions of Bi^{3+} for Sn^{4+}/Zn^{2+} can lead to the increases of the lattice constants. Even though the large difference in cation size between Bi^{3+} and Sn^{4+}/Zn^{2+}, the substitution ratio reaches larger value (7 mol%, the